

p53-dependent chemokine production by senescent tumor cells supports NKG2D-dependent tumor elimination by natural killer cells

Alexandre Iannello,^{1,2} Thornton W. Thompson,^{1,2} Michele Ardolino,^{1,2}
Scott W. Lowe,³ and David H. Raulet^{1,2}

¹Department of Molecular and Cell Biology, and ²Cancer Research Laboratory, University of California at Berkeley, Berkeley, CA 94720

³Memorial Sloan-Kettering Cancer Center, New York, NY 10065

The induction of cellular senescence is an important mechanism by which p53 suppresses tumorigenesis. Using a mouse model of liver carcinoma, where cellular senescence is triggered *in vivo* by inducible p53 expression, we demonstrated that NK cells participate in the elimination of senescent tumors. The elimination of senescent tumor cells is dependent on NKG2D. Interestingly, p53 restoration neither increases ligand expression nor increases the sensitivity to lysis by NK cells. Instead, p53 restoration caused tumor cells to secrete various chemokines with the potential to recruit NK cells. Antibody-mediated neutralization of CCL2, but not CCL3, CCL4 or CCL5, prevented NK cell recruitment to the senescent tumors and reduced their elimination. Our findings suggest that elimination of senescent tumors by NK cells occurs as a result of the cooperation of signals associated with p53 expression or senescence, which regulate NK cell recruitment, and other signals that induce NKG2D ligand expression on tumor cells.

CORRESPONDENCE
David H. Raulet:
raulet@berkeley.edu

Cellular senescence is an established cellular stress response, primarily acting to limit the proliferative potential of cells (Collado and Serrano, 2010). It can be triggered in many cell types in response to diverse cellular damage (Collado and Serrano, 2010). An important trigger of senescence is oncogenic stress, mediated by activation of p53/p21 and p16/Rb tumor suppressor pathways, which promote senescence by transactivating genes that arrest cell cycle progression and promote the senescent state (Serrano et al., 1997; Narita et al., 2003; Braig et al., 2005; Michaloglou et al., 2005; Ventura et al., 2007). It is believed that senescence is a key mechanism by which p53 suppresses tumorigenesis (Braig and Schmitt, 2006; Collado and Serrano, 2010). The senescent state is associated with several phenotypic alterations, including the secretion of soluble factors involved in the maintenance of the senescent state (e.g., CXCL2 [Acosta et al., 2008], PAI-1 [plasminogen activator inhibitor-1; Kortlever et al., 2006], IGFBP7 [insulin-like growth factor-binding protein 7; Wajapeyee et al., 2008]), and other molecules

that regulate the immune response (cytokines and chemokines; Kuilman et al., 2008; Rodier et al., 2009, 2011), angiogenesis (vascular endothelial growth factor), and other processes (Coppé et al., 2006). This so-called senescence-associated secretory phenotype (SASP), as well as the resulting immune responses, could promote or repress cancer progression in a context-dependent manner (Rodier and Campisi, 2011). With respect to immune responses, the senescent state has similarly been associated with alterations that promote tumorigenesis (Krtolica et al., 2001; Bavik et al., 2006; Yang et al., 2006; Liu and Hornsby, 2007) but in other cases with immune-mediated tumor elimination (Xue et al., 2007; Krizhanovsky et al., 2008; Kang et al., 2011).

Accumulating evidence suggests that immune-mediated destruction of senescent cells

© 2013 Iannello et al. This article is distributed under the terms of an Attribution-Noncommercial-Share Alike-No Mirror Sites license for the first six months after the publication date (see <http://www.rupress.org/terms>). After six months it is available under a Creative Commons License (Attribution-Noncommercial-Share Alike 3.0 Unported license, as described at <http://creativecommons.org/licenses/by-nc-sa/3.0/>).

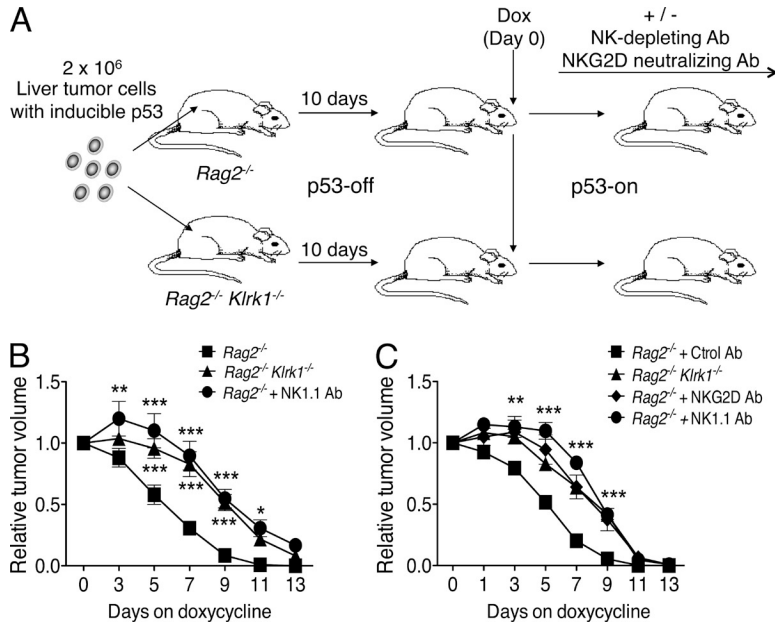


Figure 1. NKG2D-dependent elimination of senescent tumors by NK cells. (A) *Rag2^{-/-}*, *Rag2^{-/-}Klrk1^{-/-}*, and NK-depleted *Rag2^{-/-}* mice ($n = 6$ to 11 per group) were injected subcutaneously with 2×10^6 liver tumor cells with inducible p53. 10 d after injection, tumor sizes were measured and doxycycline was added to the drinking water. This day was designated day 0. Tumor sizes were monitored 3, 5, 7, 9, 11, and 13 d later. (B) Relative tumor volumes (day 0 = 1) for each group of mice are shown. Values represent mean \pm SEM for each group. Two-way ANOVA and Bonferroni's tests were performed at each time point. The data depict combined data from two independent experiments. (C) *Rag2^{-/-}* and *Rag2^{-/-}Klrk1^{-/-}* mice were injected subcutaneously with 2×10^6 liver tumor cells and treated as described in A. NK depletion and NKG2D blocking were performed in some groups by intraperitoneal injection of 200 μ g NK1.1 or NKG2D antibodies, respectively. Tumor sizes were monitored 1, 3, 5, 7, 9, 11, and 13 d after doxycycline treatment. Relative tumor volumes for each group of mice are shown ($n = 5$ mice per group). The data depict combined data from two independent experiments. Values represent means \pm SEM for each group. Two-way ANOVA and Bonferroni's tests were performed at each time point. *, $P < 0.05$; **, $P < 0.01$; ***, $P < 0.001$.

may play a role in tumor surveillance as well as in resolution of fibrotic injury to tissues (Xue et al., 2007; Krizhanovsky et al., 2008; Kang et al., 2011; Lujambio et al., 2013). In some cases, immune cells such as NK cells and other immune effector cells like granulocytes and macrophages have been implicated in mediating these effects (Xue et al., 2007; Krizhanovsky et al., 2008; Lujambio et al., 2013).

NK cells are lymphocytes that kill tumor cells and infected cells and secrete various inflammatory cytokines, including IFN- γ and TNF (Vivier et al., 2011). Like other lymphocytes and immune cells, NK cells are recruited to infected or transformed tissue by the action of chemokine gradients (Grégoire et al., 2007). NK cell killing requires engagement of specific ligands on tumor cells by NK receptors. Some NK receptors, specific for MHC I molecules, inhibit NK activity, whereas other receptors activate NK functions (Vivier et al., 2011). Several activating NK receptors have been implicated in the killing of tumor cells. The best characterized such receptor is NKG2D (encoded by the *Klrk1* gene), which is expressed by all NK cells. NKG2D binds to each of 5–10 (depending on the individual) different MHC I-related cell surface ligands, including the RAE-1/MULT1/H60 subfamilies of proteins in mice and the MICA/ULBP subfamilies of proteins in humans (Raulet, 2003). The ligands are expressed poorly by normal cells but are often induced on cancer cells as the result of stress pathways or other pathways that are dysregulated in cancer cells (Raulet et al., 2013). NKG2D has been implicated in immune surveillance of tumors using transgenic models of spontaneous cancer as well as subcutaneous tumor transfer models (Cerwenka et al., 2001; Diefenbach et al., 2001; Guerra et al., 2008).

A recent paper suggested that senescent tumors are targeted for elimination by NK cells and other innate effector cells (Xue et al., 2007). However, it is unknown how p53-expressing

senescent tumors mobilize the natural killer cell response. Nor is it known how NK cells recognize the senescent tumors. In this study, we sought to define how NK cells carry out this function by defining the receptors and ligands involved and the alterations in senescent cells that mobilize the NK cell response. Our results demonstrate that induced expression of p53 in a model of transferred liver tumor cells causes the production of various chemokines, including CCL2, and that CCL2 is essential for robust recruitment of NK cells into the tumor. The NK-dependent component of tumor cell elimination is completely dependent on NKG2D-mediated recognition of RAE-1 proteins expressed on the tumor cells, but RAE-1 expression is not induced by p53 expression because it is robust on the tumor cells even before p53 expression is induced. The results suggest that other types of signals associated with the transformed state induce expression of NKG2D ligands, but p53 expression mobilizes effective NK-dependent tumor elimination by inducing CCL2 expression that recruits NK cells into the tumor.

RESULTS

NK- and NKG2D-dependent elimination of senescent tumors

We used a mouse model of tumor senescence where p53 expression in H-RasV12-transformed liver carcinoma cells (TRE_shp53 cells) is regulated by an inducible p53 shRNA, which can be extinguished in response to doxycycline (Xue et al., 2007). Hence, tumors initiated under conditions of p53 repression can be allowed to progress or can be induced by doxycycline to express p53 and hence undergo senescence *in vivo* (Xue et al., 2007). Using this system, it was previously reported that when tumors lacking p53 expression were first established in T cell-deficient nude mice, subsequent induction of p53 with doxycycline resulted in the arrest of tumor growth and the gradual disappearance of the senescent tumors

(Xue et al., 2007). Notably, the elimination of the senescent tumors was prevented or delayed when NK cells, macrophages, or granulocytes were depleted individually from the host animals at the time of doxycycline treatment (Xue et al., 2007).

In our experiments, transformed liver tumor cells were transferred subcutaneously to B6-*Rag2*^{-/-} mice, which lack T cells and B cells. p53 induction resulted in the arrest and gradual disappearance of the tumors (Fig. 1). Depletion of NK cells with NK1.1 antibody early before and after inducing p53 resulted in a significant delay in tumor elimination compared with mice treated with control IgG, corroborating the role of NK cells in the elimination of senescent tumors (Fig. 1). The tumors were still eliminated at later time points, suggesting that other mechanisms independently cause tumor elimination. These latter mechanisms may depend on neutrophils and/or macrophages (Xue et al., 2007). In subsequent experiments, we focused on the role of NK cells in the rapid elimination of senescent tumors.

To test the role of NKG2D in elimination of senescent tumors, transformed liver tumor cells were transferred subcutaneously to mice lacking both RAG2 and NKG2D (*Rag2*^{-/-} *Klrk1*^{-/-}) as well as to control *Rag2*^{-/-} (*Klrk1*^{+/+}) mice. After treatment of the mice with doxycycline, senescent tumor elimination was delayed in *Rag2*^{-/-} *Klrk1*^{-/-} mice, to a similar extent as was observed in mice depleted of NK cells (Fig. 1). A similar delay was observed in *Rag2*^{-/-} mice that were injected with NKG2D antibodies to block ligand recognition (Fig. 1 C). Furthermore, these delays were of a similar magnitude as occurred in mice depleted of NK cells, the only known cells to express NKG2D in *Rag2*^{-/-} mice. Therefore, these data demonstrate that NKG2D plays an essential role in the rapid elimination of senescent tumors by NK cells.

p53 restoration is not necessary for expression of NKG2D ligands in the liver tumor cells

The finding that NKG2D plays a role in eliminating senescent tumors led us to investigate the possibility that p53 expression or the senescent state is associated with the induced expression of NKG2D ligands. Transformed fetal liver cells cultivated in vitro in the p53-off state expressed substantial amounts of one NKG2D ligand, RAE-1 ϵ , but did not express MULT1 or H60 family ligands (Fig. 2 A). Cultivation of these cells in vitro with doxycycline for 7 d did not result in a significantly increased expression of any of the NKG2D ligands at either the protein level (as shown by staining with ligand-specific antibodies or by staining with NKG2D-Fc, which binds to all NKG2D ligands; Fig. 2 A) or mRNA level (Fig. 2 C). Induction of p53 in vivo, in established tumors implanted in *Rag2*^{-/-} *Klrk1*^{-/-} recipients, also did not result in consistent or significantly increased expression of RAE-1 ϵ (Fig. 2, B and D) or other NKG2D ligands (Fig. 2 A and not depicted), as shown by ex vivo analysis of tumor cell suspensions. These data suggest that RAE-1 expression occurs without p53 induction in this model and that p53 restoration and/or the senescent state do not further induce the expression of NKG2D ligands.

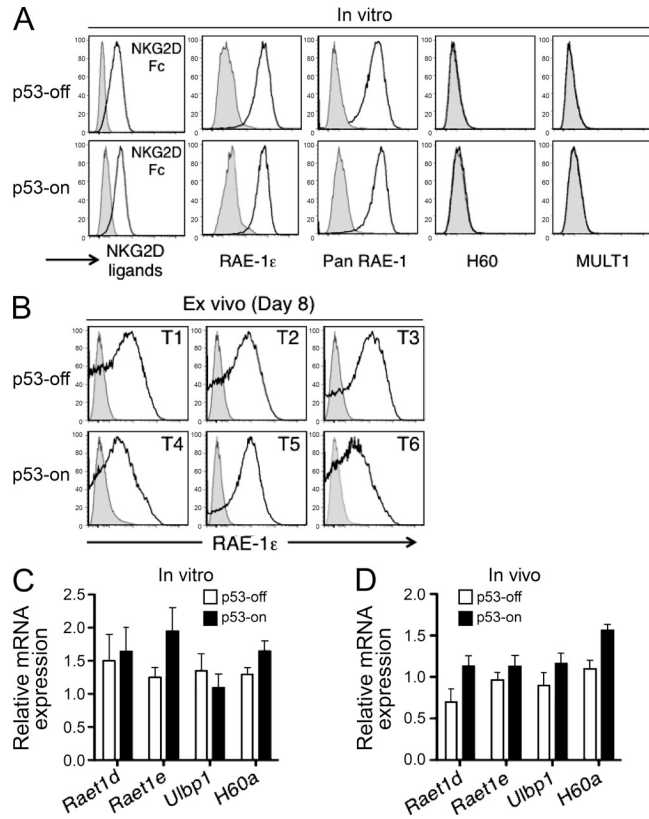


Figure 2. NKG2D ligand expression on tumor cells. (A) NKG2D ligand expression on tumor cells cultivated in vitro for 7 d without (p53-off) and with (p53-on) doxycycline. The data are representative of at least three independent experiments. (B) RAE-1 ϵ expression under p53-off versus p53-on conditions by tumor cells established in *Rag2*^{-/-} *Klrk1*^{-/-} mice, 8 d after initiating treatment with doxycycline. Three representative tumors from each group are shown. (C) Liver tumor cells were cultivated in vitro as described in A. After 7 d, cells were harvested, RNA prepared, and transcripts encoding NKG2D ligands were quantified by Q-RT-PCR. Histograms represent the relative abundance of various NKG2D ligand mRNAs in p53-on versus p53-off tumors. mRNA amounts were normalized to the 18S rRNA reference. None of the differences between p53-on and p53-off groups were statistically significant. Values represent means \pm SEM from three independent experiments. (D) Established tumors in *Rag2*^{-/-} mice were treated or not with doxycycline. 8 d later, tumors were harvested, and single cell suspensions of tumors were processed as described in C. mRNA amounts were normalized to the 18S rRNA reference. None of the differences between p53-on and p53-off groups were statistically significant. Values represent means \pm SEM from three independent experiments.

Although p53 expression was not associated with increased expression of NKG2D ligands, it remained possible that the induction of senescence rendered the cells more susceptible to NKG2D-dependent lysis. As shown in Fig. 3 A, however, p53-restoration and the accompanying senescence did not increase the sensitivity of the tumor cells to killing by IL-2-activated NK cells in vitro; if anything, killing was slightly reduced. The killing of the tumor cells in vitro, whether they expressed p53 or not, was nevertheless largely NKG2D dependent, as it was much reduced when the NK cells were derived from *Klrk1*^{-/-} mice (Fig. 3 B). Similarly,

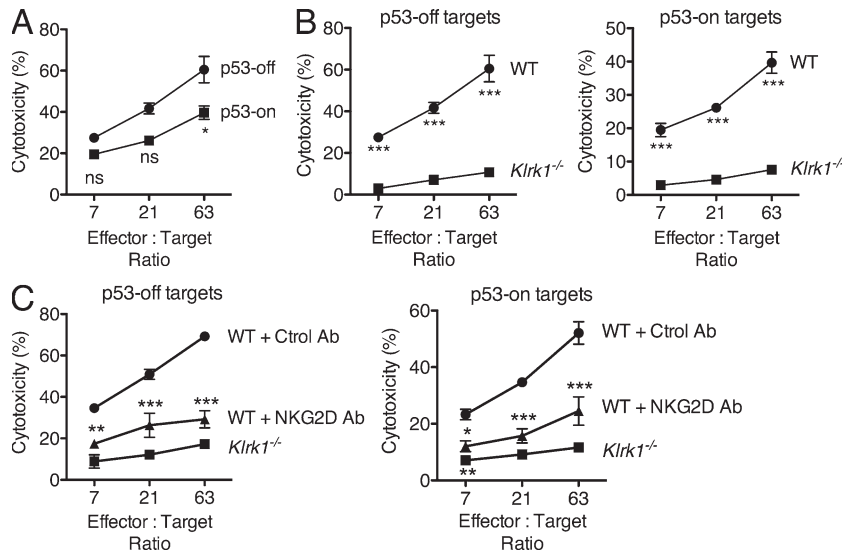


Figure 3. NKG2D-dependent killing of proliferating and senescent tumor cells. (A) Lysis by IL-2-activated NK cells of p53-off versus p53-on tumor cells (day 7 after cultivating the cells in doxycycline). Significance was tested with two-way ANOVA and Bonferroni's tests at each effector to target ratio. Values represent means \pm SEM for each effector to target ratio. (B) Lysis of p53-off and p53-on target cells by WT versus *Klrk1*^{-/-} IL-2-activated NK cells. Values represent means \pm SEM for each effector to target ratio. The data presented in A and B are representative of three independent experiments. (C) Lysis by IL-2-activated NK cells of p53-off versus p53-on tumor cells (day 7 after cultivating the cells in doxycycline) in the presence or absence of 50 μ g/ml NKG2D Ab (clone MI-6) to block the interaction. The significance of the differences between the MI-6-treated groups compared with the control groups was tested with two-way ANOVA and Bonferroni's tests at each effector to target ratio. Values represent means \pm SEM for each effector to target ratio. The data presented are representative of two independent experiments. Note that error bars are presented throughout but are in some cases smaller than the symbols. * $P < 0.05$; ** $P < 0.01$; *** $P < 0.001$.

blocking NKG2D with antibodies to prevent ligand recognition resulted in a significant decrease in the sensitivity of the tumor cells to killing by NK cells in vitro (Fig. 3 C). Therefore, although p53 restoration did not induce or increase the expression of NKG2D ligands, the elimination of p53-restored tumor cells was dependent on NKG2D recognition by NK cells, as tested by in vitro killing (Fig. 3) or tumor rejection in vivo (Fig. 1).

A subsequent investigation of tumor cell phenotypes in vivo provided another line of evidence that NKG2D plays a role in elimination of the senescent tumor cells. As already noted, p53 restoration did not cause a change of RAE-1 ϵ expression in tumors implanted in *Rag2*^{-/-}/*Klrk1*^{-/-} mice (Fig. 2 B). In *Rag2*^{-/-} mice, in contrast, p53 restoration for 8 d resulted in a reproducible reduction in the expression of RAE-1 ϵ on tumor cells (Fig. 4, A and B). The reduction was not observed in *Rag2*^{-/-}/*Klrk1*^{-/-} control recipients, or in *Rag2*^{-/-} mice that were depleted of NK cells (Fig. 4, A and B). Furthermore, the reduction in RAE-1 ϵ expression did not occur in *Rag2*^{-/-} mice when the tumors were not induced to express p53 (Fig. 4 B). These data suggested that p53 expression facilitates NK cell-dependent tumor cell killing in vivo, resulting in the preferential elimination of tumor cells expressing high levels of the NK activating ligand RAE-1 ϵ .

p53 restoration is associated with increased chemokine expression and NK cell recruitment

Having observed no effect of p53 on expression of NKG2D ligands or sensitivity of tumor cells to NK-mediated lysis in vitro, we considered the possibility that p53 expression might either enhance NK cell accumulation in the tumor or the activity of the NK cells once within the tumor. To address

NK cell accumulation, established tumors in *Rag2*^{-/-} mice (p53-on or -off) were harvested at different time points after beginning doxycycline treatment, and cell suspensions were stained to quantify tumor-infiltrating CD45 $^+$ immune cells as well as CD45 $^+$ NKp46 $^+$ NK cells by flow cytometry (Fig. 5). Importantly, p53 restoration induced a progressive accumulation of immune (CD45 $^+$) cells in the tumors, which was not observed in tumors that did not express p53 (Fig. 5 A). Most of the recruited CD45 $^+$ cells were various myeloid cells, but the percentage of the CD45 $^+$ cells that were NK cells increased dramatically over the same time course in a p53-dependent fashion (Fig. 5 B) and the percentage of NK cells among all cells in the tumor suspension increased strikingly as a result (Fig. 5 C). Importantly, the accumulation of CD45 $^+$ cells in general, and of NK cells in particular, was not dependent on NKG2D, as it occurred equally in *Rag2*^{-/-} and *Rag2*^{-/-}/*Klrk1*^{-/-} mice (Fig. 5, D and E). Even with this sharp increase, only \sim 2% of tumor infiltrates were NK cells, but these cells were essential for rapid rejection of the tumors as shown in Fig. 1. These data demonstrate a key role mediated by p53 in the intratumoral accumulation of immune cells, especially NK cells.

The accumulation of immune cells in infected tissues or tumors is often the result of recruitment of the cells by gradients of locally produced specific chemokines. We therefore investigated whether p53 restoration in these liver tumor cells induces the secretion of various chemokines. A large panel of cytokines and chemokines were investigated both in vitro and in vivo after p53 induction. In vitro, restoration of p53 in transformed fetal liver cells resulted in significant increases in the mRNAs for several chemokines known to recruit immune cells, including CCL2, CCL4, and CCL5 (Fig. 6 A).

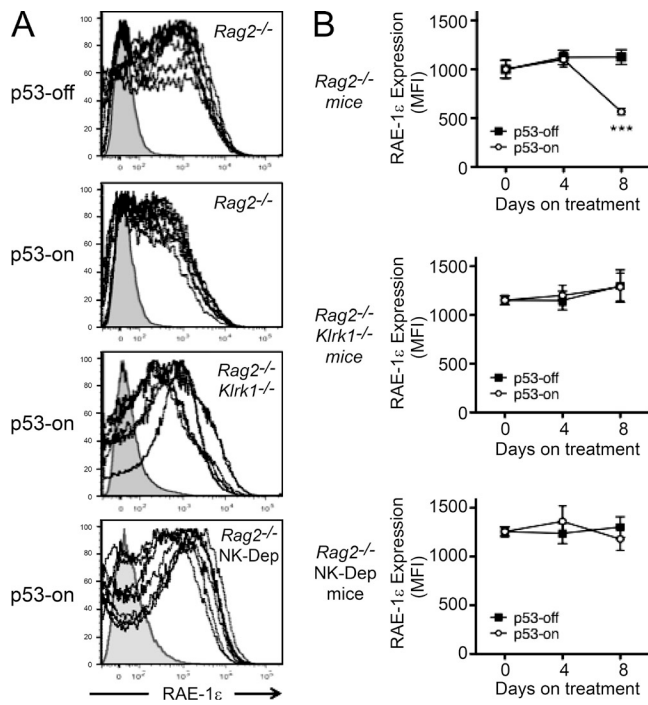
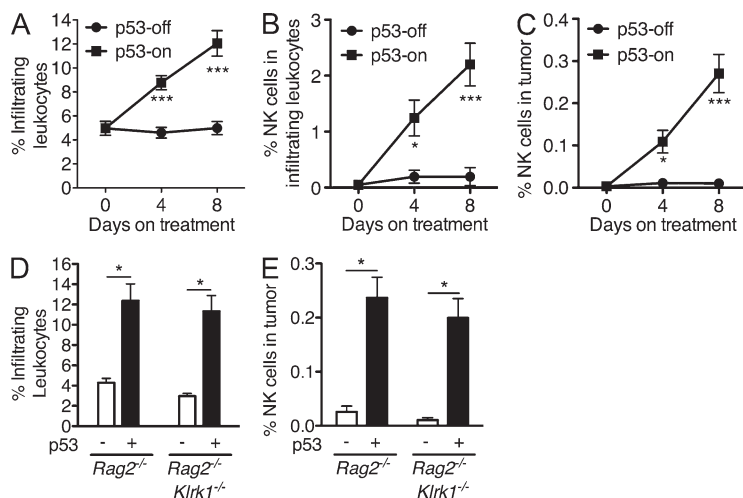


Figure 4. RAE-1 ϵ expression on ex vivo tumor cells. (A) Ex vivo RAE-1 ϵ cell surface expression 8 d after restoring p53 expression, or not, on tumors implanted in *Rag2 $^{-/-}$* , *Rag2 $^{-/-}$ Klrk1 $^{-/-}$* , and *Rag2 $^{-/-}$* mice depleted of NK cells (NK-Dep). For each panel, a representative isotype staining (filled gray histogram) was overlaid with $n = 7$ tumor stainings for RAE-1 ϵ (dotted black lines). The figure depicts combined data from two independent experiments. (B) Graphical depiction of RAE-1 ϵ cell surface expression with or without p53 induction in *Rag2 $^{-/-}$* , *Rag2 $^{-/-}$ Klrk1 $^{-/-}$* , and NK-depleted *Rag2 $^{-/-}$* hosts ($n = 7$ mice per group). The graphs depict averages of the mean fluorescence intensities (MFIs) of RAE-1 ϵ staining on day 0 (before doxycycline treatment), and on days 4 and 8 after beginning treatment, or not, with doxycycline. Values represent means \pm SEM for each group ($n = 7$). Error bars are in some cases smaller than the symbols. Two-way ANOVA and Bonferroni's tests were performed at each time point. The figure depicts combined data from two independent experiments. ***, P < 0.001.



A comparable analysis of ex vivo tumor samples from mice treated or not with doxycycline showed a similar induction of mRNAs for these chemokines and several others, including CCL3, CXCL1, and CXCL2 (Fig. 6 B). Many of these changes were confirmed at the protein level using protein arrays (Fig. 6 C).

We next investigated which cells (tumor or immune cells) were producing these soluble factors in vivo when p53 was restored. The transformed tumor cells, which express GFP, were used for tumor implantation in mice. Established tumors were harvested (p53-off and -on) and single cell suspensions of the tumors were stained with CD45 antibodies to stain all hematopoietic cells within the tumor. CD45 $^{+}$ cells and GFP $^{+}$ cells (tumor cells) were sorted by flow cytometry and tested by Q-RT-PCR. mRNAs for the CC-chemokines CCL2, CCL3, CCL4, and CCL5 and the CXC-chemokines CXCL1 and CXCL2 were found to be up-regulated in GFP $^{+}$ tumor cells (Fig. 6 D) after p53 expression in vivo (Fig. 6 E). Some up-regulation of the same chemokines may also occur in CD45 $^{+}$ hematopoietic cells in the tumors (Fig. 6 F), but the combined data from three experiments failed to reach statistical significance.

Published chromatin immunoprecipitation experiments show a direct association of p53 with the *Ccl2* gene regulatory sequences (Hacke et al., 2010; Tang et al., 2012), which is consistent with the possibility that p53 directly transactivates *Ccl2*. Furthermore, the Ct values from the Q-RT-PCR experiments suggested that the tumors produced greater amounts of CCL2 than of the other chemokines tested (unpublished data). To confirm the generality of *Ccl2* induction in senescent cells by p53, we transduced WT or *Trip53 $^{-/-}$* (p53 KO) MEFs with H-RasV12 and cultured the cells for 8 d (Fig. 7 A). These experiments were based on a previous study (Brady et al., 2011) showing that H-RasV12 induces senescence in MEFs that express the wild-type form of p53.

Figure 5. p53-induced senescence increases natural killer cell infiltration into the tumors. (A–C) *Rag2 $^{-/-}$* mice were injected subcutaneously with 2×10^6 liver tumor cells with inducible p53. 10 d later, tumors were harvested from one group of mice (day 0), whereas other groups continued with (p53-on) or without (p53-off) doxycycline treatment for an additional 4 or 8 d. Single cell tumor suspensions were stained with CD45 and NKp46 antibodies to determine the percentages of infiltrating hematopoietic cells (CD45 $^{+}$) among all cells in the tumors (A), the percentages of NK cells (NKp46 $^{+}$) among the infiltrating hematopoietic cells (B), and the percentage of NK cells among all cells in the tumors. The data are representative of two to three independent experiments. (D and E) Established tumors in *Rag2 $^{-/-}$* or *Rag2 $^{-/-}$ Klrk1 $^{-/-}$* mice were treated or not with doxycycline. 8 d later, single cell tumor suspensions were stained as described in A–C to determine the percentages of infiltrating CD45 $^{+}$ cells among all cells in the tumors (D) and the percentages of NK cells among all cells in the tumors (E). Values represent means \pm SEM ($n = 8$ mice per group for A and 5 mice per group for B–E). Two-way ANOVA and Bonferroni's tests were performed. The data are representative of two to three independent experiments. *, P < 0.05; ***, P < 0.001.

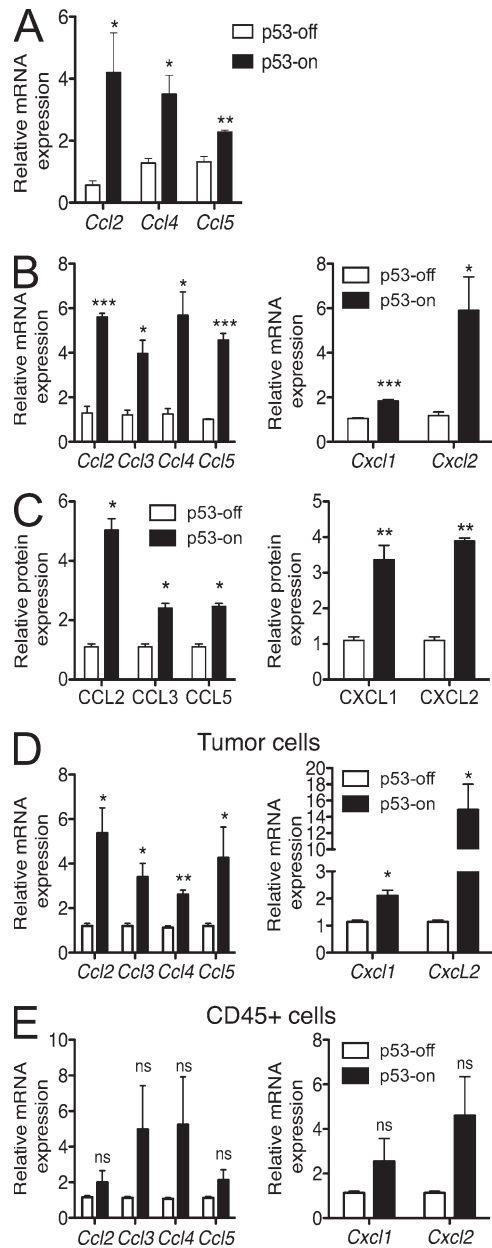


Figure 6. p53 restoration induces production of numerous chemokines by cells in the tumors. (A) Liver tumor cells were cultivated in vitro with or without 100 ng/ml doxycycline. After 7 d, cells were harvested, RNA prepared, and transcripts encoding various chemokines were quantified by Q-RT-PCR. Histograms represent the relative abundance of chemokine mRNAs in p53-on tumors versus p53-off tumors. mRNA amounts were normalized to the 18S rRNA reference. Values represent means \pm SEM for each target. The data are representative of at least three independent experiments. (B and C) Established tumors in *Rag2^{-/-}* mice were treated or not with doxycycline. 8 d later, tumors were harvested, and single cell suspensions of tumors were processed as described in A for quantification of mRNAs (B), or lysates were prepared and used to quantify the relative amounts of various chemokine proteins using a protein array (C). Histograms represent the relative abundance of various mRNAs or proteins in p53-on tumors versus p53-off tumors 8 d after beginning treatment with doxycycline. Values represent means \pm SEM for each target. The data are representative of three independent experiments. (D and E) Established tumors in *Rag2^{-/-}* mice were prepared as in B, and tumor cell suspensions were fractionated into CD45⁻GFP⁺ tumor cells (D; note that the tumor cells express GFP) and CD45⁻GFP⁻ infiltrating hematopoietic cells (E) by fluorescence activated cell sorting after staining with CD45 antibodies. The populations were processed for Q-RT-PCR as in A, to quantify various chemokine transcripts. mRNA amounts were normalized to the 18S rRNA reference. Student's *t* tests were performed for each transcript, comparing p53-off versus p53-on groups. Values represent means \pm SEM from three independent experiments. *, P < 0.05; **, P < 0.01; ***, P < 0.001.

Similar to the results with liver tumor cells, a fourfold increase in *Ccl2* gene expression was observed in WT MEFs transduced with H-RasV12 (Fig. 7 B). In contrast, H-RasV12 transduction induced much less *Ccl2* mRNA in p53 KO MEFs, suggesting that p53 plays a critical role in inducing *Ccl2* gene expression (Fig. 7 B). The *Ccl2* induction was also confirmed at the protein level by ELISA performed on the cell culture supernatants. As shown in Fig. 7 C, the amount of CCL2 protein secreted by H-RasV12-transduced WT MEFs was much higher than the amount secreted by H-RasV12-transduced p53 KO MEF.

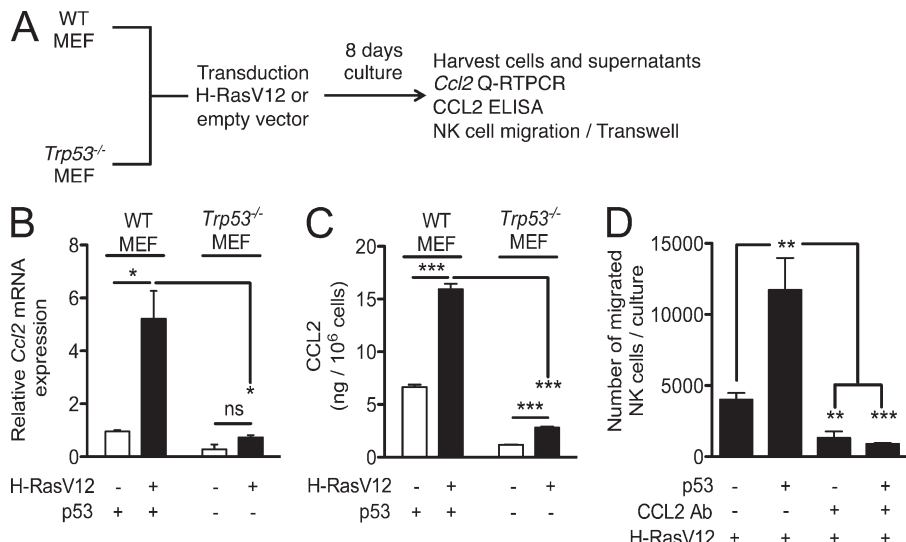
We next investigated the potential role of the secreted CCL2 in the migration of NK cells in vitro, using a transwell system. As shown in Fig. 7 D, H-RasV12-transduced p53-expressing senescent MEFs strongly induced the migration of IL-2-activated NK cells. The migration was blocked when neutralizing CCL2-specific polyclonal antibodies were included in the cultures, demonstrating the role of CCL2 in the observed migration. Importantly, much less migration occurred with H-RasV12-transduced, p53 KO MEF. These data indicate the importance of p53 in the migration process by virtue of its activity in inducing CCL2 production.

Neutralization of CCL2 prevents NK cell recruitment in vivo and diminishes tumor cell rejection

NK cells can be rapidly recruited to sites of infection or inflammation due to expression of various chemokine receptors, including CCR2, CCR5, CXCR3, and CX3CR1 (Grégoire et al., 2007; Walzer and Vivier, 2011). CCR2 is the receptor for CCL2, whereas CCR5 is the receptor for CCL3, 4, and 5. To test the role of these chemokines in leukocyte recruitment and subsequent tumor clearance, mice with implanted tumors were treated with doxycycline and simultaneously treated with control IgG, a neutralizing antibody for CCL2, or a cocktail of neutralizing antibodies for CCL3, CCL4, and CCL5 (Fig. 8). These antibodies have been shown to be effective in neutralizing the corresponding chemokines in published experiments (Martinez de la Torre et al., 2007; Pace et al., 2012).

8 d after administering the antibodies, the percentages of various CD45⁺ cell types in the tumors were determined. Neutralizing CCL2 caused a striking reduction in the recruitment of NK cells into the tumors, whereas neutralizing CCL3, CCL4, and CCL5 had no such effect (Fig. 8, A and B). The reduction was apparent when NK cell content was expressed

ments. (D and E) Established tumors in *Rag2^{-/-}* mice were prepared as in B, and tumor cell suspensions were fractionated into CD45⁻GFP⁺ tumor cells (D; note that the tumor cells express GFP) and CD45⁻GFP⁻ infiltrating hematopoietic cells (E) by fluorescence activated cell sorting after staining with CD45 antibodies. The populations were processed for Q-RT-PCR as in A, to quantify various chemokine transcripts. mRNA amounts were normalized to the 18S rRNA reference. Student's *t* tests were performed for each transcript, comparing p53-off versus p53-on groups. Values represent means \pm SEM from three independent experiments. *, P < 0.05; **, P < 0.01; ***, P < 0.001.



p53-off versus p53-on groups. Histograms represent means and standard errors of three independent experiments. (D) Migration of IL-2-activated NK cells induced by H-RasV12-expressing WT or p53 KO MEF, with or without the addition of CCL2 antibodies or control rabbit IgG. One-way ANOVA and Tukey's comparison tests were performed on groups. Histograms represent means and standard errors of three independent experiments. *, P < 0.05; **, P < 0.01; ***, P < 0.001.

as the percentage of CD45⁺ cells (Fig. 8 A) or as the percentage of all cells in the tumor (Fig. 8 B). In contrast, neutralizing CCL2 (or CCL3, CCL4, and CCL5) had no significant effect on the recruitment of various myeloid cells, including granulocytes

(F4/80⁻ Ly6G⁺ CD11b⁺ Ly6C⁺ CD11c⁻), inflammatory monocytes (F4/80⁺ Ly6G⁻ CD11b⁺ Ly6C^{high} CD11c⁻), or monocytes/macrophages (F4/80⁺ Ly6G⁻ CD11b⁺ Ly6C^{low} CD11c⁺; Fig. 8, A and B), and consequently did not significantly

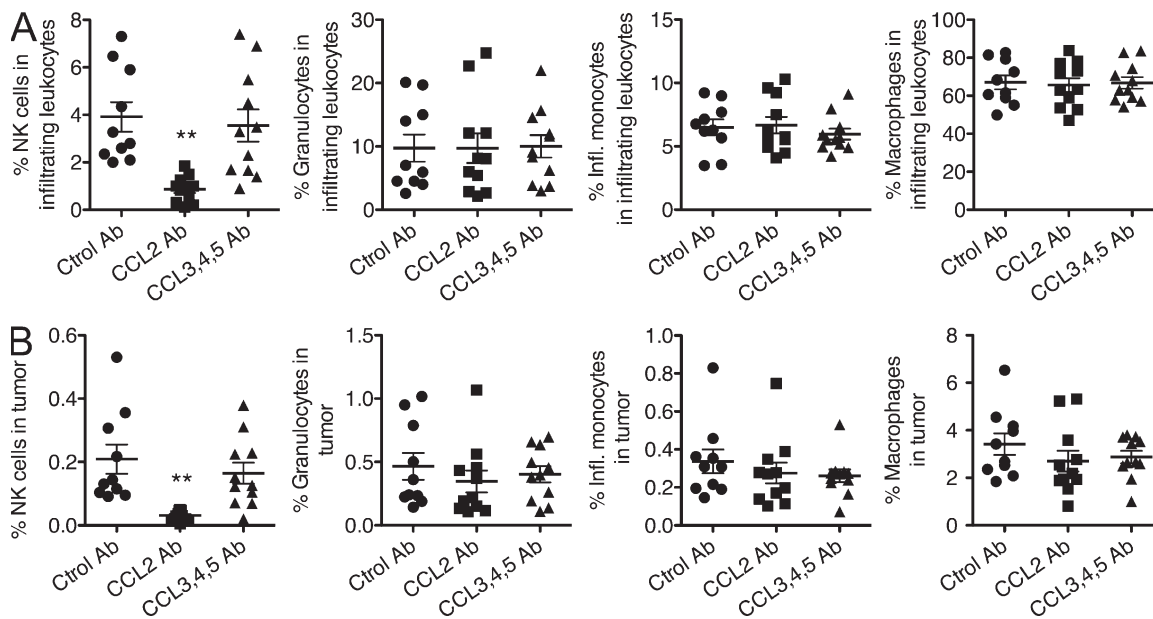


Figure 8. CCL2 neutralization inhibits natural killer cell infiltration into senescent tumors. *Rag2*^{-/-} mice were injected subcutaneously with 2×10^6 liver tumor cells with inducible p53. 10 d after injection (day 0), tumor sizes were measured and doxycycline treatment was initiated. In vivo neutralization of CCL2, or of CCL3, 4, and 5 was performed by intraperitoneal injection of 100 μ g CCL2 antibodies or a cocktail of 100 μ g each of CCL3, CCL4, and CCL5 antibodies. Injections were performed on days 0 and 4 of doxycycline treatment. Control mice were injected with rat IgG (Ctrl Ab). Tumors were harvested on day 8, and single cell tumor suspensions examined by staining and flow cytometry to quantify the percentages of NKP46⁺ NK cells, granulocytes (F4/80⁻ Ly6G⁺ CD11b⁺ Ly6C⁺ CD11c⁻), inflammatory monocytes (F4/80⁺ Ly6G⁻ CD11b⁺ Ly6C^{high} CD11c⁻), and monocytes/macrophages (F4/80⁺ Ly6G⁻ CD11b⁺ Ly6C^{low} CD11c⁺). Data are presented as percentages of CD45⁺ cells (A) or percentages of all cells in the tumor (B). n = 10–11 mice per group. Comparison of the groups by one-way ANOVA and Tukey's multiple comparison tests showed that the difference in NK cell infiltration between the CCL2 neutralized and control group was significant, P < 0.01. The data depict combined data from two independent experiments, which each gave similar results. Horizontal lines represent the means for each group. **, P < 0.01.

alter the percentage of total CD45⁺ cells in the tumors (not depicted). These data indicate that CCL2 plays an important and nonredundant role in recruitment of NK cells into senescent tumors, supporting the conclusion that induced expression of CCL2 as a result of p53 expression enhances CCL2-dependent NK cell recruitment to the tumors.

Importantly, the neutralization of CCL2 not only inhibited NK cell recruitment into the tumors, it also delayed the rejection of senescent tumor cells *in vivo*, as shown by parallel monitoring of tumor sizes after initiating p53 restoration and antibody treatments (Fig. 9). The delay in tumor elimination was significant though not as robust as the delay that occurred in mice treated with NK1.1 antibodies to deplete NK cells. Collectively, the data support the conclusion that induction of CCL2 expression as a result of p53 restoration substantially enhanced NK cell recruitment to tumors, as well as NK cell–dependent elimination of tumor cells mediated by NKG2D interactions.

In addition to the effects of p53 on chemokine expression, the expression data we obtained suggested a role of p53 in the induction of cytokines that are known to activate NK cells (Fig. 10). Thus, p53 restoration resulted in enhanced expression, at both the mRNA and protein levels, of IL-15, IL12p40, IL-18, IL-1, and IL-6 in ex vivo samples of tumors in which p53 expression was restored (Fig. 10, B and C). Analysis of separated tumor cells and infiltrating CD45⁺ cells indicated that IL-12, IL-15, and IL-1, at least, were induced significantly in tumor cells, whereas IL-6 was probably produced

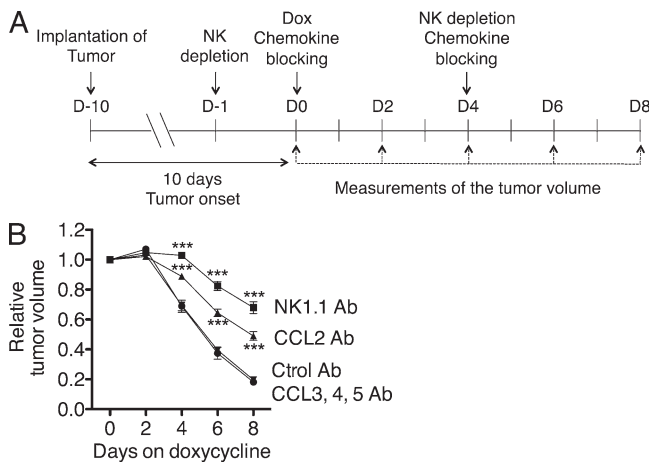


Figure 9. CCL2 neutralization delays the elimination of senescent tumors. (A) Tumors were initiated, treated with doxycycline to induce p53, and treated with NK-depleting antibodies (NK1.1), neutralizing chemokine-specific antibodies, or control antibodies as shown in A. (B) The relative volumes of the tumors (day 0 = 1) were monitored on the days shown. Values represent means \pm SEM for each group (error bars are in some cases smaller than the symbols). Comparisons of the groups by two-way ANOVA and Bonferroni's tests showed that the difference between the CCL2-neutralized and control group was significant, $P < 0.001$ at days 4, 6, and 8. The data depict combined data from two independent experiments, which each gave similar results. ***, $P < 0.001$.

by CD45⁺ cells (Fig. 10 D). Of the cytokines that were induced in senescent tumor cells, at least IL-15 and IL-12 + IL-18 (which act synergistically) are known to be potent activators of NK cells. Hence, cytokines induced in senescent tumors may enhance NK cell activation within the tumors, aiding in tumor elimination.

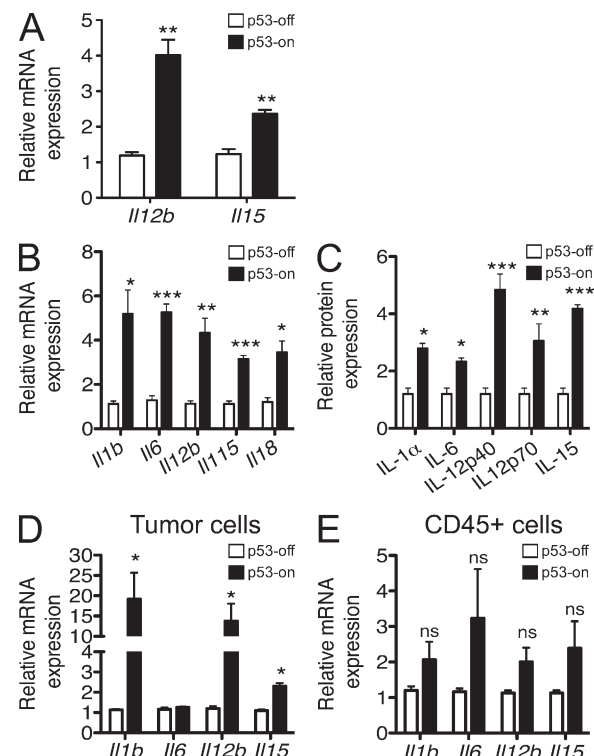


Figure 10. p53 restoration induces production of numerous cytokines by cells in the tumors. (A) Liver tumor cells were cultivated in vitro with or without 100 ng/ml doxycycline. After 7 d, cells were harvested, RNA prepared, and transcripts encoding various cytokines were quantified by Q-RT-PCR. mRNA amounts were normalized to the 18S rRNA reference. Histograms represent the relative abundance of cytokine mRNAs in p53-on tumors versus p53-off tumors. Values represent means \pm SEM for each target. The data are representative of at least three independent experiments. (B and C) Established tumors in *Rag2*^{-/-} mice were treated or not with doxycycline. 8 d later, tumors were harvested, and single cell suspensions of tumors were processed as described in A (B), or lysates were used to quantify the relative amounts of various cytokine proteins using a protein array (C). Histograms represent the relative abundance of various mRNAs or proteins in p53-on tumors versus p53-off tumors 8 d after initiating treatment with doxycycline. mRNA amounts were normalized to the 18S rRNA reference. Values represent means \pm SEM for each target. The data are representative of three independent experiments. (D and E) Established tumors in *Rag2*^{-/-} mice were prepared as in B and tumor cell suspensions were stained with CD45 antibodies before sorting CD45⁻GFP⁺ tumor cells (D) and CD45^{+GFP}⁻ infiltrating hematopoietic cells (E). The populations were processed for Q-RT-PCR as in A, to quantify various cytokine transcripts. mRNA amounts were normalized to the 18S rRNA reference. Student's *t* tests were performed comparing p53-off versus p53-on histograms for each target. Values represent means \pm SEM from three independent experiments. *, $P < 0.05$; **, $P < 0.01$; ***, $P < 0.001$. ns, not significant.

DISCUSSION

In this study, we have investigated the mechanistic basis of extrinsic immune-mediated tumor suppression associated with cellular senescence. Previous studies from our laboratory demonstrated that transplanted tumor cells expressing NKG2D ligands are rejected by NK cells and, in some cases, T cells (Diefenbach et al., 2000, 2001, 2003), and that knockout mice lacking NKG2D display an enhanced incidence and/or more rapid onset of cancers in certain mouse models of spontaneous cancer (Guerra et al., 2008). Published studies showed that NK cells, via granule exocytosis, play a major role in eliminating tumors that become senescent (Xue et al., 2007; Sagiv et al., 2013). Here, we demonstrated that NKG2D-mediated recognition is largely if not exclusively responsible for the NK cell-dependent component of senescent liver tumors. The activation of tumor elimination mechanisms by senescent tumors may benefit the host in three respects: by reducing the likelihood that variant tumor cells lacking p53 can arise from the senescent tumor mass, by facilitating the elimination of passenger nonsenescent tumor cells in the tumor mass, and by preventing the senescent tumor cells from exerting protumorigenic effects on neighboring tissues (Krtolica et al., 2001; Parrinello et al., 2005; Coppé et al., 2006, 2008; Liu and Hornsby, 2007; Laberge et al., 2012).

Considering NKG2D's role, it might have been expected that NKG2D ligands would be increased in senescent tumors compared with growing tumors. We observed instead that p53 restoration did not increase RAE-1 expression above the already high level we observed in growing tumor cells. These findings are consistent with previous studies suggesting that NKG2D ligands are induced by a variety of other stimuli, including E2F transcription factors, PI3 kinase, Ras oncogene signaling, and an activated DNA damage response (Gasser et al., 2005; Tokuyama et al., 2011; Jung et al., 2012). We had previously concluded that p53 does not play a major role in the expression of NKG2D ligands, at least in the mouse cells tested. In contrast, two studies reported that pharmacological reactivation of p53 in specific cell lines can stimulate the expression of ULPB2, a ligand for human NKG2D (Li et al., 2011; Textor et al., 2011). Hence, p53 may in some cases enhance NKG2D ligand expression, but it appears that it plays other, possibly more important, roles in facilitating NKG2D-dependent elimination of tumors, as documented in this paper.

The main phenotype observed after p53 restoration in vivo was a nearly threefold overall increase in the percentage of immune cells within the tumor, including an increase of ~20-fold in the percentage of NK cells in the tumors. The accumulation of immune cells was independent of NKG2D. Consistent with a role for senescence in recruiting immune cells, another study showed that mouse livers harboring premalignant senescent hepatocytes showed an inflammatory reaction with large clusters of immune cells surrounding senescent hepatocytes (Kang et al., 2011). Several cytokines (including CCL2) were directly secreted by the senescent hepatocytes. This study correlated the presence of these soluble factors with immune surveillance and infiltration by immune

cells (Kang et al., 2011), but direct evidence for their participation was not provided.

Senescent cells and cells expressing p53 communicate with their environment in part by secreting various cytokines, chemokines, and growth factors. We propose that these chemokines play a critical role in the immune surveillance of senescent tumor cells by NK cells and possibly other immune cells. We observed a strong induction of various important chemokines, as well as NK cell-activating interleukins including IL-12 and IL-15 after p53 induction in vitro and in vivo. Our data suggest that some of these chemokines and cytokines were produced directly by senescent tumor cells, whereas tumor-infiltrating immune cells also produced some of these cytokines/chemokines and in one case were probably the exclusive source of a cytokine (IL-6). We were, however, unable to detect IFN- γ production in NK cells extracted from the tumors by flow cytometry, or by using protein arrays with extracts of whole tumors. We also did not observe an increase in IFN- γ mRNA, as examined by Q-RT-PCR analysis of either whole tumor extracts or extracts of tumor-infiltrating CD45 $^{+}$ cells. These data suggest that the steady-state amounts of IFN- γ produced by NK cells in the tumor are low, lessening the likelihood that increases in IFN- γ production play a major role in tumor rejection in this model.

Although p53-expressing senescent tumors secreted several chemokines with the potential to recruit NK cells, the in vitro migration experiments and in vivo antibody neutralization studies presented herein suggest that CCL2 plays a predominant role in this process. CCL2 was first identified as a monocyte attractant, but evidence has accumulated that it can recruit other cells including memory T cells and dendritic cells. It has been implicated in NK cell recruitment before but has not stood out as the major chemokine for recruiting these cells (Grégoire et al., 2007). The *Ccl2* gene, which may be directly transactivated by p53 (Hacke et al., 2010; Tang et al., 2012), was induced in liver tumor cells as a result of p53 restoration and in p53-expressing but not *Trp53*-KO MEFs transduced with H-RasV12 (Fig. 6, D and E; and Fig. 7, B and C, respectively). In fact, calculations of the relative amounts of CCL2 mRNA in liver tumor cells versus hematopoietic cells of ex vivo tumor cells, which take into account the greater abundance of transformed versus hematopoietic cells in the tumors, suggest that tumor cells account for >85% of the CCL2 transcripts (unpublished data). The p53-dependence of CCL2 production may distinguish CCL2 from some of the other chemokines produced in senescent cells, which are dependent on the senescent state but are produced independently of p53 (Coppé et al., 2008; Rodier et al., 2009). The latter chemokines are among the mediators associated with the so-called senescence-associated secretory phenotype (SASP), some of which have protumorigenic activities.

An interesting feature of our findings is that p53 expression did not enhance NKG2D ligand expression or the sensitivity of the tumor cells to NK lysis, but instead functioned by boosting the recruitment of NK cells to the tumor, and potentially the activation state of the NK cells that reached the

tumors. These findings may be one explanation for why expression of NKG2D ligands in some cancers is insufficient to trigger NKG2D-dependent elimination of tumors (Jinushi et al., 2003; Guerra et al., 2008; McGilvray et al., 2009; Hilpert et al., 2012). In the case of the liver tumor cells studied here, for example, a high level of RAE-1 on the cells was insufficient to cause elimination of the tumor cells. p53 restoration both stalled the growth of the cells and caused the increased recruitment of NK cells that aided in tumor elimination. Hence, stress-induced signals that induce NKG2D ligands and senescence-specific signals that recruit and activate NK cells can cooperate in affecting the elimination of senescent tumors and possibly other senescent tissues *in vivo*.

Our findings that p53 acts in part by enhancing the recruitment and activation of NK cells has the additional implication that p53 may also, in some cases, enhance rejection of tumors by NKG2D-independent recognition mechanisms. Depending on the ligands expressed by the tumor cells studied, different NK-activating receptors may be engaged and trigger cytotoxicity (Vivier et al., 2011). Thus, it is plausible that enhanced recruitment and activation of NK cells resulting from p53 expression is important for rejection of tumor cells that express those ligands, as well as for tumors that express NKG2D ligands.

Our results suggest the importance of p53 expression and senescence in immune surveillance at the early stages of tumorigenesis before p53 is inactivated or lost due to mutation. Conversely, an implication of our findings is that loss of p53 function and/or the bypass of senescence, which occurs in the majority of advanced tumors, can impair immune surveillance of tumors by decreasing the efficiency of NK cell recruitment within the tumor. Methods that restore these p53-mediated functions might therefore be fruitful in enhancing NK cell-mediated tumor elimination (Nardella et al., 2011). Given that the mediators act to recruit NK cells, it might be sufficient to restore p53 activity in only a fraction of the tumor cells in a given tumor to achieve a beneficial effect.

Additional analysis of the senescence-associated events that underlie immune surveillance of premalignant senescent cells is clearly warranted. Further studies are needed to elucidate the different senescence-dependent signals provided by tumor cells that will converge to create a cancer-associated pattern needed to trigger immune surveillance. Understanding and characterizing the mechanisms of senescence surveillance such as the secretory phenotype and the regulation of immune cell effector functions is clearly a new research direction in the senescence field. This line of investigation may uncover new strategies for therapeutic augmentation of immune responses against a broad variety of cancers in the future.

MATERIALS AND METHODS

Mice and *in vivo* procedures. *Rag2^{-/-}* and *Klrk1^{-/-}* (NKG2D KO) mice were both on the C57BL6 background. The NKG2D KO mouse strain is available at The Jackson Laboratory Repository with the JAX Stock No. 022733. *Rag2^{-/-}* and *Klrk1^{-/-}* mice were intercrossed to generate *Rag2^{-/-}*–*Klrk1^{-/-}* mice. The *Klrk1* knockout genotypes were determined by genomic PCR (Guerra et al., 2008). To generate subcutaneous tumors, 2×10^6 liver

tumor cells were subcutaneously injected into the rear flanks of the mice. Tumor volume (in cubic millimeters) was determined by caliper measurement and calculated as length \times width² \times $\pi/6$. All animal procedures were performed according to the National Institutes of Health guidelines under protocols approved by the University of California Animal Care and Use Committee.

For NK cell depletion *in vivo*, mice were injected i.p. with 200 μ g NK1.1 antibodies (clone PK136) for two consecutive days before doxycycline treatment and every 4 d thereafter once doxycycline treatment was initiated. For blocking chemokines *in vivo*, mice were injected i.p. with 100 μ g CCL2 polyclonal antibodies or a cocktail (100 μ g for each Ab) of CCL3 (clone 39624), CCL4 (clone 46907), and CCL5 (clone 53405) antibodies (all from R&D Systems). Injections were performed 1 d before doxycycline treatment and on day 4 after initiation of doxycycline treatment.

Cells, antibodies, and reagents. The liver tumor cells (named TRE_shp53) used in this study were previously reported (Xue et al., 2007). Cell cultures were performed at 37°C in humidified atmosphere containing 5% CO₂. Liver tumor cells and MEFs were cultivated in DMEM with 10% FCS, 100 U/ml penicillin, 100 μ g/ml streptomycin, 0.2 mg/ml glutamine, 10 μ g/ml gentamycin sulfate, and 20 mM Hepes (referred to below as complete medium). For *in vitro* experiments, cells were cultured in 100 ng/ml doxycycline (Sigma-Aldrich) in complete DMEM medium and the medium was refreshed every 2 d. *In vivo*, the drinking water was supplemented with 0.2 mg/ml doxycycline in 0.5% sucrose solution, kept in light-protected bottles, and refreshed every 4 d. IL-2-activated NK cells were prepared by incubating wild-type and *Klrk1^{-/-}* C57BL6 splenocytes for 5 d in RPMI complete medium with 1,000 U/ml recombinant human IL-2 (National Cancer Institute).

The NKG2D (MI-6) and NK1.1 (PK136) antibodies were prepared and purified in house. The following Abs were purchased from R&D Systems: anti-RAE-1 ϵ (clone 205001), anti-panRAE-1 (clone 186107), anti-H60 (polyclonal Ab), and APC-conjugated anti-MULT1 (clone 237104). From eBioscience, we purchased biotinylated anti-NKp46 (clone 29A1.4), streptavidin (SA)-APC and SA-PECy7, APC-conjugated anti-CD45.1 (clone A20), PercPCy5.5-conjugated anti-Ly6C (clone HK1.4), PE-conjugated anti-F4/80 (clone BM8), and PECy7-conjugated anti-CD11c (clone N418). From BioLegend, we purchased APC-conjugated anti-NKp46 (clone 29A1.4), BV605-conjugated anti-CD11b (clone M1/70), AF700-conjugated anti-Ly6G (clone 1A8), and APC-conjugated anti-human IgG Fc (clone HP6017). Propidium iodide and CountBright absolute counting beads were purchased from Invitrogen.

Flow cytometry. Cells cultivated *in vitro* were preincubated for 20 min on ice with PBS containing 2.4G2 antibodies to block Fc receptors. Between incubations (and before analysis), cells were washed with PBS containing 0.05% BSA and 0.002% sodium azide. For the first staining step, cells were incubated for 30 min on ice with antibodies conjugated with biotin or fluorochromes. Cells were incubated with fluorochrome-conjugated streptavidin for 30 min on ice when necessary. For staining *ex vivo* cells, fresh tumor tissues were excised from mice, minced, and dissociated using the gentleMACS Dissociator (Miltenyi Biotec). Dissociated tumor samples were further digested in DMEM containing 200 μ g/ml Collagenase IV (Roche) and 20 μ g/ml DNase I (Sigma-Aldrich) at 37°C for 45 min. After filtering through a 70- μ m nylon mesh, single cell suspensions were stained as described above. Flow cytometry was performed with an LSRII or LSRFortessa flow cytometer (BD). FACSDiva software was used for acquisition of data and FlowJo software was used for analysis (BD).

NK cell cytotoxicity assay. NK cell cytotoxicity was determined with a standard 4-h ⁵¹Cr-release assay. In brief, 10⁴ ⁵¹Cr-labeled TRE_shp53 cells were dispensed in 100 μ l of culture medium in quadruplicates in the wells of V-bottomed 96-well plates. IL-2-activated NK cells were added in 100 μ l of culture medium to each well to achieve effector-to-target cell ratios of 9:1, 27:1, or 81:1. For NKG2D blocking *in vitro*, IL-2-activated NK cells were incubated with 100 μ g NKG2D Ab (clone MI-6) for 30 min at room

temperature before adding to target cells. The microcultures were incubated for 4 h at 37°C in a humidified 5% CO₂ atmosphere, after which the plates were centrifuged and 40 µl of the culture supernatants were collected and mixed with 180 µl OPTIPHASE SUPERMIX (PerkinElmer). The radiation in each sample was counted with an automated β counter (Microbeta TriLux; PerkinElmer). The spontaneous release was in all cases <20% of the maximum release accomplished with detergent. The percentage of specific ⁵¹Cr-release was calculated according to the following formula: % specific lysis = 100 × (experimental – spontaneous release)/(detergent release – spontaneous release).

RNA isolation, reverse transcription, and quantitative PCR. Total RNA was isolated using the RNeasy Mini kit (QIAGEN), and treated with DNaseI (DNA-free kit; Invitrogen) for 25 min at 37°C. For comparisons among samples, an equal amount of RNA was reverse transcribed to cDNA using the iScript reverse transcription system (Bio-Rad Laboratories) according to the manufacturer's instructions. Quantitative real-time PCR was performed using SSO-Fast EvaGreen Supermix (Bio-Rad Laboratories) on a CFX96 thermocycler (Bio-Rad Laboratories), according to the manufacturer's instructions. mRNA amounts were normalized to amplifications of the reference 18S rRNA and are plotted as relative expression values. The primers used for Q-RT-PCR analyses are listed in Table S1.

Protein arrays. Single cell suspension from ex vivo tumors were obtained as described above and lysed on ice. Cytokines and chemokines in cell lysates were quantified using customized membrane-based protein arrays (RayBiotech Inc.), according to the manufacturer's instructions. The signals on the membranes were revealed by autoradiography using x-ray film. Autoradiographs were scanned and the images were quantified by densitometric analysis using the ImageJ software.

NK cell migration assay. MEFs from WT or *Tp53*^{-/-} C57BL/6 mice were transduced with pBABE puro H-RasV12 or pBABE puro (empty vector) plasmids and selected with 2 µg/ml puromycin for 8 d. After 8 d of culture, H-RasV12-expressing WT or *p53* KO MEFs were seeded in the bottom chamber of a transwell system (6.5-mm diameter inserts and 5.0-µm pore size; Corning) for 24 h. In parallel, IL-2-activated NK cells were generated with spleen cells from NCR-GFP mice (provided by O. Mandelboim, The Hebrew University of Jerusalem, Jerusalem, Israel). GFP⁺ NK cells were sorted on the day of the assay (5 d after culturing with IL-2) and seeded in the upper chamber of the transwell system. CCL2 (R&D Systems) or 50 µg/ml control antibodies were added 30 min before seeding NK cells in the upper chamber. The co-culture was incubated at 37°C for 4 h. After 4 h, nonadherent cells from the bottom chamber were harvested, washed, and resuspended in 200 µl PBS in 96-well V-bottom plates, and a known number of fluorescent counting beads (in a volume of 10 µl) was added to each well. A volume of 200 µl/well was analyzed by flow cytometry and the absolute number of GFP⁺ NK cells in 200 µl was calculated using this formula: A*(B/C), where A = number of NK cell events, B = the number of beads added to each culture, and C = number of bead events.

Statistical analysis. Statistical comparisons were performed with the Prism software (GraphPad Software). P-values were determined using ANOVA (one- and two-way tests) or unpaired Student's *t* tests (two-tailed). Differences between groups were considered significant for p-values <0.05.

Online supplemental material. Table S1 shows a list of forward and reverse primers used in Q-RT-PCR and the amplicon size for each target. Online supplemental material is available at <http://www.jem.org/cgi/content/full/jem.20130783/DC1>.

We thank R. Vance, L. Coscoy, and L. He for critical comments on the manuscript. We thank Lin He for providing WT and *Tp53* KO MEFs and the members of the Raulet laboratory for discussions, suggestions, and advice. We thank L. Zhang for managing the laboratory, and H. Nolla and A. Valeros for valuable assistance with flow cytometry.

This work was supported by grant R01 AI039642 from the National Institutes of Health to D.H. Raulet. A. Iannello was supported by the Canadian Institutes for Health Research (CIHR) Banting postdoctoral scholarship. M. Ardolino was supported by an Institut Pasteur-Fondazione Cenci Bolognetti postdoctoral scholarship.

The authors declare no competing financial interests.

A. Iannello and D.H. Raulet designed the research and experiments; A. Iannello performed experiments; T.W. Thompson and M. Ardolino helped in performing experiments and contributed to their interpretation; S.W. Lowe provided the TRE_shp53 cells and contributed to interpretation and discussion of the results; T.W. Thompson and M. Ardolino helped in writing the manuscript; and A. Iannello and D.H. Raulet interpreted the results, prepared the figures, and wrote the final version of the manuscript.

Submitted: 15 April 2013

Accepted: 12 August 2013

REFERENCES

- Acosta, J.C., A. O'Loughlin, A. Banito, M.V. Guijarro, A. Augert, S. Raguz, M. Fumagalli, M. Da Costa, C. Brown, N. Popov, et al. 2008. Chemokine signaling via the CXCR2 receptor reinforces senescence. *Cell*. 133:1006–1018. <http://dx.doi.org/10.1016/j.cell.2008.03.038>
- Bavik, C., I. Coleman, J.P. Dean, B. Knudsen, S. Plymate, and P.S. Nelson. 2006. The gene expression program of prostate fibroblast senescence modulates neoplastic epithelial cell proliferation through paracrine mechanisms. *Cancer Res.* 66:794–802. <http://dx.doi.org/10.1158/0008-5472.CAN-05-1716>
- Brady, C.A., D. Jiang, S.S. Mello, T.M. Johnson, L.A. Jarvis, M.M. Kozak, D. Kenzelmann Broz, S. Basak, E.J. Park, M.E. McLaughlin, et al. 2011. Distinct p53 transcriptional programs dictate acute DNA-damage responses and tumor suppression. *Cell*. 145:571–583. <http://dx.doi.org/10.1016/j.cell.2011.03.035>
- Braig, M., and C.A. Schmitt. 2006. Oncogene-induced senescence: putting the brakes on tumor development. *Cancer Res.* 66:2881–2884. <http://dx.doi.org/10.1158/0008-5472.CAN-05-4006>
- Braig, M., S. Lee, C. Loddenkemper, C. Rudolph, A.H. Peters, B. Schlegelberger, H. Stein, B. Dörken, T. Jenuwein, and C.A. Schmitt. 2005. Oncogene-induced senescence as an initial barrier in lymphoma development. *Nature*. 436:660–665. <http://dx.doi.org/10.1038/nature03841>
- Cerwenka, A., J.L. Baron, and L.L. Lanier. 2001. Ectopic expression of retinoic acid early inducible-1 gene (RAE-1) permits natural killer cell-mediated rejection of a MHC class I-bearing tumor in vivo. *Proc. Natl. Acad. Sci. USA*. 98:11521–11526. <http://dx.doi.org/10.1073/pnas.201238598>
- Collado, M., and M. Serrano. 2010. Senescence in tumours: evidence from mice and humans. *Nat. Rev. Cancer*. 10:51–57. <http://dx.doi.org/10.1038/nrc2772>
- Coppé, J.P., K. Kauser, J. Campisi, and C.M. Beauséjour. 2006. Secretion of vascular endothelial growth factor by primary human fibroblasts at senescence. *J. Biol. Chem.* 281:29568–29574. <http://dx.doi.org/10.1074/jbc.M603307200>
- Coppé, J.P., C.K. Patil, F. Rodier, Y. Sun, D.P. Muñoz, J. Goldstein, P.S. Nelson, P.Y. Desprez, and J. Campisi. 2008. Senescence-associated secretory phenotypes reveal cell-nonautonomous functions of oncogenic RAS and the p53 tumor suppressor. *PLoS Biol.* 6:2853–2868. <http://dx.doi.org/10.1371/journal.pbio.0060301>
- Diefenbach, A., A.M. Jamieson, S.D. Liu, N. Shastri, and D.H. Raulet. 2000. Ligands for the murine NKG2D receptor: expression by tumor cells and activation of NK cells and macrophages. *Nat. Immunol.* 1:119–126. <http://dx.doi.org/10.1038/77793>
- Diefenbach, A., E.R. Jensen, A.M. Jamieson, and D.H. Raulet. 2001. Rae1 and H60 ligands of the NKG2D receptor stimulate tumour immunity. *Nature*. 413:165–171. <http://dx.doi.org/10.1038/35093109>
- Diefenbach, A., J.K. Hsia, M.Y. Hsiung, and D.H. Raulet. 2003. A novel ligand for the NKG2D receptor activates NK cells and macrophages and induces tumor immunity. *Eur. J. Immunol.* 33:381–391. <http://dx.doi.org/10.1002/immu.200310012>
- Gasser, S., S. Orsulic, E.J. Brown, and D.H. Raulet. 2005. The DNA damage pathway regulates innate immune system ligands of the NKG2D receptor. *Nature*. 436:1186–1190. <http://dx.doi.org/10.1038/nature03884>

- Grégoire, C., L. Chasson, C. Luci, E. Tomasello, F. Geissmann, E. Vivier, and T. Walzer. 2007. The trafficking of natural killer cells. *Immunol. Rev.* 220:169–182. <http://dx.doi.org/10.1111/j.1600-065X.2007.00563.x>
- Guerra, N., Y.X. Tan, N.T. Joncker, A. Choy, F. Gallardo, N. Xiong, S. Knoblaugh, D. Cado, N.M. Greenberg, and D.H. Raulet. 2008. NKG2D-deficient mice are defective in tumor surveillance in models of spontaneous malignancy. *Immunity*. 28:571–580. <http://dx.doi.org/10.1016/j.jimmuni.2008.02.016>
- Hacke, K., B. Rincon-Orozco, G. Buchwalter, S.Y. Siehler, B. Waslylyk, L. Wiesmüller, and F. Rösl. 2010. Regulation of MCP-1 chemokine transcription by p53. *Mol. Cancer*. 9:82. <http://dx.doi.org/10.1186/1476-4598-9-82>
- Hilpert, J., L. Grosse-Hovest, F. Grünebach, C. Buechle, T. Nuebling, T. Raum, A. Steinle, and H.R. Salih. 2012. Comprehensive analysis of NKG2D ligand expression and release in leukemia: implications for NKG2D-mediated NK cell responses. *J. Immunol.* 189:1360–1371. <http://dx.doi.org/10.4049/jimmunol.1200796>
- Jinushi, M., T. Takehara, T. Tatsumi, T. Kanto, V. Groh, T. Spies, R. Kimura, T. Miyagi, K. Mochizuki, Y. Sasaki, and N. Hayashi. 2003. Expression and role of MICA and MICB in human hepatocellular carcinomas and their regulation by retinoic acid. *Int. J. Cancer*. 104:354–361. <http://dx.doi.org/10.1002/ijc.10966>
- Jung, H., B. Hsiung, K. Pestal, E. Procyk, and D.H. Raulet. 2012. RAE-1 ligands for the NKG2D receptor are regulated by E2F transcription factors, which control cell cycle entry. *J. Exp. Med.* 209:2409–2422. <http://dx.doi.org/10.1084/jem.20120565>
- Kang, T.W., T. Yevsa, N. Woller, L. Hoenicke, T. Wuestefeld, D. Dauch, A. Hohmeyer, M. Gereke, R. Rudalska, A. Potapova, et al. 2011. Senescence surveillance of pre-malignant hepatocytes limits liver cancer development. *Nature*. 479:547–551. <http://dx.doi.org/10.1038/nature10599>
- Kortlever, R.M., P.J. Higgins, and R. Bernards. 2006. Plasminogen activator inhibitor-1 is a critical downstream target of p53 in the induction of replicative senescence. *Nat. Cell Biol.* 8:877–884. <http://dx.doi.org/10.1038/ncb1448>
- Krizhanovsky, V., M. Yon, R.A. Dickins, S. Hearn, J. Simon, C. Miethling, H. Yee, L. Zender, and S.W. Lowe. 2008. Senescence of activated stellate cells limits liver fibrosis. *Cell*. 134:657–667. <http://dx.doi.org/10.1016/j.cell.2008.06.049>
- Krtolica, A., S. Parrinello, S. Lockett, P.Y. Desprez, and J. Campisi. 2001. Senescent fibroblasts promote epithelial cell growth and tumorigenesis: a link between cancer and aging. *Proc. Natl. Acad. Sci. USA*. 98:12072–12077. <http://dx.doi.org/10.1073/pnas.211053698>
- Kuilman, T., C. Michaloglou, L.C. Vredeveld, S. Douma, R. van Doorn, C.J. Desmet, L.A. Aarden, W.J. Mooi, and D.S. Peepur. 2008. Oncogene-induced senescence relayed by an interleukin-dependent inflammatory network. *Cell*. 133:1019–1031. <http://dx.doi.org/10.1016/j.cell.2008.03.039>
- Laberge, R.M., P. Awad, J. Campisi, and P.Y. Desprez. 2012. Epithelial-mesenchymal transition induced by senescent fibroblasts. *Cancer Micro-environ.* 5:39–44. <http://dx.doi.org/10.1007/s12307-011-0069-4>
- Li, H., T. Lakshminikanth, C. Garofalo, M. Enge, C. Spinnler, A. Anichini, L. Szekely, K. Kärre, E. Carbone, and G. Selivanova. 2011. Pharmacological activation of p53 triggers anticancer innate immune response through induction of ULBP2. *Cell Cycle*. 10:3346–3358. <http://dx.doi.org/10.4161/cc.10.19.17630>
- Liu, D., and P.J. Hornsby. 2007. Senescent human fibroblasts increase the early growth of xenograft tumors via matrix metalloproteinase secretion. *Cancer Res.* 67:3117–3126. <http://dx.doi.org/10.1158/0008-5472.CAN-06-3452>
- Lujambio, A., L. Akkari, J. Simon, D. Grace, D.F. Tschaharganeh, J.E. Bolden, Z. Zhao, V. Thapar, J.A. Joyce, V. Krizhanovsky, and S.W. Lowe. 2013. Non-cell-autonomous tumor suppression by p53. *Cell*. 153:449–460. <http://dx.doi.org/10.1016/j.cell.2013.03.020>
- Martinez de la Torre, Y., C. Buracchi, E.M. Borroni, J. Dupor, R. Bonecchi, M. Nebuloni, F. Pasqualini, A. Doni, E. Lauri, C. Agostinis, et al. 2007. Protection against inflammation- and autoantibody-caused fetal loss by the chemokine decoy receptor D6. *Proc. Natl. Acad. Sci. USA*. 104:2319–2324. <http://dx.doi.org/10.1073/pnas.0607514104>
- McGilvray, R.W., R.A. Eagle, N.F. Watson, A. Al-Attar, G. Ball, I. Jafferji, J. Trowsdale, and L.G. Durrant. 2009. NKG2D ligand expression in human colorectal cancer reveals associations with prognosis and evidence for immunoediting. *Clin. Cancer Res.* 15:6993–7002. <http://dx.doi.org/10.1158/1078-0432.CCR-09-0991>
- Michaloglou, C., L.C. Vredeveld, M.S. Soengas, C. Denoyelle, T. Kuilman, C.M. van der Horst, D.M. Majoor, J.W. Shay, W.J. Mooi, and D.S. Peepur. 2005. BRAFE600-associated senescence-like cell cycle arrest of human nevi. *Nature*. 436:720–724. <http://dx.doi.org/10.1038/nature03890>
- Nardella, C., J.G. Clohessy, A. Alimonti, and P.P. Pandolfi. 2011. Pro-senescence therapy for cancer treatment. *Nat. Rev. Cancer*. 11:503–511. <http://dx.doi.org/10.1038/nrc3057>
- Narita, M., S. Núñez, E. Heard, M. Narita, A.W. Lin, S.A. Hearn, D.L. Spector, G.J. Hannan, and S.W. Lowe. 2003. Rb-mediated heterochromatin formation and silencing of E2F target genes during cellular senescence. *Cell*. 113:703–716. [http://dx.doi.org/10.1016/S0092-8674\(03\)00401-X](http://dx.doi.org/10.1016/S0092-8674(03)00401-X)
- Pace, L., A. Tempez, C. Arnold-Schrauf, F. Lemaitre, P. Bousso, L. Fettler, T. Sparwasser, and S. Amigorena. 2012. Regulatory T cells increase the avidity of primary CD8+ T cell responses and promote memory. *Science*. 338:532–536. <http://dx.doi.org/10.1126/science.1227049>
- Parrinello, S., J.P. Coppe, A. Krtolica, and J. Campisi. 2005. Stromal-epithelial interactions in aging and cancer: senescent fibroblasts alter epithelial cell differentiation. *J. Cell Sci.* 118:485–496. <http://dx.doi.org/10.1242/jcs.01635>
- Raulet, D.H. 2003. Roles of the NKG2D immunoreceptor and its ligands. *Nat. Rev. Immunol.* 3:781–790. <http://dx.doi.org/10.1038/nri1199>
- Raulet, D.H., S. Gasser, B.G. Gowen, W. Deng, and H. Jung. 2013. Regulation of ligands for the NKG2D activating receptor. *Annu. Rev. Immunol.* 31:413–441. <http://dx.doi.org/10.1146/annurev-immunol-032712-095951>
- Rodier, F., and J. Campisi. 2011. Four faces of cellular senescence. *J. Cell Biol.* 192:547–556. <http://dx.doi.org/10.1083/jcb.201009094>
- Rodier, F., J.P. Coppé, C.K. Patil, W.A. Hoeijmakers, D.P. Muñoz, S.R. Raza, A. Freund, E. Campeau, A.R. Davalos, and J. Campisi. 2009. Persistent DNA damage signalling triggers senescence-associated inflammatory cytokine secretion. *Nat. Cell Biol.* 11:973–979. <http://dx.doi.org/10.1038/ncb1909>
- Rodier, F., D.P. Muñoz, R. Teachenor, V. Chu, O. Le, D. Bhaumik, J.P. Coppé, E. Campeau, C.M. Beauséjour, S.H. Kim, et al. 2011. DNA-SCARS: distinct nuclear structures that sustain damage-induced senescence growth arrest and inflammatory cytokine secretion. *J. Cell Sci.* 124:68–81. <http://dx.doi.org/10.1242/jcs.071340>
- Sagiv, A., A. Biran, M. Yon, J. Simon, S.W. Lowe, and V. Krizhanovsky. 2013. Granule exocytosis mediates immune surveillance of senescent cells. *Oncogene*. 32:1971–1977. <http://dx.doi.org/10.1038/onc.2012.206>
- Serrano, M., A.W. Lin, M.E. McCurrach, D. Beach, and S.W. Lowe. 1997. Oncogenic ras provokes premature cell senescence associated with accumulation of p53 and p16INK4a. *Cell*. 88:593–602. [http://dx.doi.org/10.1016/S0092-8674\(00\)81902-9](http://dx.doi.org/10.1016/S0092-8674(00)81902-9)
- Tang, X., M. Asano, A. O'Reilly, A. Farquhar, Y. Yang, and S. Amar. 2012. p53 is an important regulator of CCL2 gene expression. *Curr. Mol. Med.* 12:929–943. <http://dx.doi.org/10.2174/156652412802480844>
- Textor, S., N. Fiegler, A. Arnold, A. Porgador, T.G. Hofmann, and A. Cerwenka. 2011. Human NK cells are alerted to induction of p53 in cancer cells by upregulation of the NKG2D ligands ULBP1 and ULBP2. *Cancer Res.* 71:5998–6009. <http://dx.doi.org/10.1158/0008-5472.CAN-10-3211>
- Tokuyama, M., C. Lorin, F. Delebecque, H. Jung, D.H. Raulet, and L. Coscoy. 2011. Expression of the RAE-1 family of stimulatory NK-cell ligands requires activation of the PI3K pathway during viral infection and transformation. *PLoS Pathog.* 7:e1002265. <http://dx.doi.org/10.1371/journal.ppat.1002265>
- Ventura, A., D.G. Kirsch, M.E. McLaughlin, D.A. Tuveson, J. Grimm, L. Lintault, J. Newman, E.E. Reczek, R. Weissleder, and T. Jacks. 2007. Restoration of p53 function leads to tumour regression in vivo. *Nature*. 445:661–665. <http://dx.doi.org/10.1038/nature05541>
- Vivier, E., D.H. Raulet, A. Moretta, M.A. Caligiuri, L. Zitvogel, L.L. Lanier, W.M. Yokoyama, and S. Ugolini. 2011. Innate or adaptive immunity? The

- example of natural killer cells. *Science*. 331:44–49. <http://dx.doi.org/10.1126/science.1198687>
- Wajapeyee, N., R.W. Serra, X. Zhu, M. Mahalingam, and M.R. Green. 2008. Oncogenic BRAF induces senescence and apoptosis through pathways mediated by the secreted protein IGFBP7. *Cell*. 132:363–374. <http://dx.doi.org/10.1016/j.cell.2007.12.032>
- Walzer, T., and E. Vivier. 2011. G-protein-coupled receptors in control of natural killer cell migration. *Trends Immunol.* 32:486–492. <http://dx.doi.org/10.1016/j.it.2011.05.002>
- Xue, W., L. Zender, C. Miething, R.A. Dickins, E. Hernando, V. Krizhanovsky, C. Cordon-Cardo, and S.W. Lowe. 2007. Senescence and tumour clearance is triggered by p53 restoration in murine liver carcinomas. *Nature*. 445:656–660. <http://dx.doi.org/10.1038/nature05529>
- Yang, G., D.G. Rosen, Z. Zhang, R.C. Bast Jr., G.B. Mills, J.A. Colacino, I. Mercado-Uribe, and J. Liu. 2006. The chemokine growth-regulated oncogene 1 (Gro-1) links RAS signaling to the senescence of stromal fibroblasts and ovarian tumorigenesis. *Proc. Natl. Acad. Sci. USA*. 103:16472–16477. <http://dx.doi.org/10.1073/pnas.0605752103>